

$S - P - D$ Mixing in Vector Quarkonia from the Salpeter Equation with Optimized Wave Function Representations

Wen-Yuan Ke^{1,2,3}, Qiang Li⁴, Tianhong Wang⁵, Tai-Fu Feng^{1,2,3}, Guo-Li Wang^{1,2,3*}

¹ *Department of Physics, Hebei University, Baoding, 071002, China*

² *Hebei Key Laboratory of High-Precision Computation and Application of Quantum Field Theory, Baoding 071002, China*

³ *Hebei Research Center of the Basic Discipline for Computational Physics, Baoding 071002, China*

⁴ *School of Physical Science and Technology, Northwestern Polytechnical University, Xi'an 710072, China*

⁵ *School of Physics, Harbin Institute of Technology, Harbin 150001, China*

Abstract

This paper proposes a novel mechanism based on the instantaneous Bethe-Salpeter (Salpeter) equation for investigating wave function mixing in vector mesons such as $\psi(3770)$. Conventional theories typically treat $\psi(3770)$ as a $2S - 1D$ mixed state; however, considering only tensor forces or relativistic corrections alone often leads to mixing angles that are too small and inconsistent with experimental data. Phenomenological $2S - 1D$ mixing requires experimental data as input to determine the mixing angles, resulting in limited theoretical studies on states like $\Upsilon(1D, 2D)$ in the absence of experimental data. To more accurately describe $S - D$ mixing and its relativistic effects, this paper systematically compares eight possible relativistic wave function representations (φ_1 to φ_8) by solving the Salpeter equation and calculates the mass spectra and dileptonic decay widths of charmonium and bottomonium. The study finds that the wave function representation φ_2 can simultaneously reproduce the experimental data of both charmonium and bottomonium well. Further analysis reveals that, in addition to $S - D$ mixing, the wave functions of vector mesons contain a non-negligible P -wave component, meaning they are $S - P - D$ mixed states. We predict the mixing angles for bottomonium $\Upsilon(1D)$ and $\Upsilon(2D)$ to be $(1.78^{+0.32})^\circ$ and $(5.44^{+1.10})^\circ$, with dileptonic decay widths of $2.29^{+0.86}_{-0.69}$ eV and $10.5^{+4.2}_{-3.1}$ eV, respectively.

* corresponding author

I. INTRODUCTION

The $\psi(3770)$ is a vector charmonium primarily dominated by the D -wave with a small S -wave admixture. It was experimentally discovered in 1977 [1]. However, before its discovery, theoretical predictions had indicated that the tensor force between quarks, which does not conserve orbital angular momentum, would lead to $S - D$ mixing [2]. Beside the tensor-force, coupled-channel effects can also account for the $S - D$ mixing [3, 4]. Consequently, 1^- mesons with the same quark composition all have the potential to mix, including highly excited states [4–7]. Since the masses of the $\psi(2S)$ and $\psi(3770)$ are close, their mixing is maximal [2]. It is therefore widely accepted that $\psi(2S)$ and $\psi(3770)$ are $2S - 1D$ mixing states. The mixing formula is

$$\begin{aligned} |\psi(2S)\rangle &= \cos \theta |2^3S_1\rangle - \sin \theta |1^3D_1\rangle, \\ |\psi(3770)\rangle &= \sin \theta |2^3S_1\rangle + \cos \theta |1^3D_1\rangle. \end{aligned} \quad (1)$$

The $S - D$ mixing nature of $\psi(3770)$ has been confirmed experimentally. The decay rate of a pure D -wave state into dileptons is extremely small, vanishing in the non-relativistic limit. The admixture of an S -wave component significantly enhances the decay width, making it experimentally observable [1]. Subsequently, the mixing properties of $\psi(3770)$ have attracted substantial research interest [8, 9]. Further study finds that the naive picture of $\psi(3770)$ as a simple $1D - 2S$ mixed state is unsatisfactory. Many theories predict a mixing angle around $|\theta| = 10^\circ$; for example, Ref. [10] gives 10° , Ref. [11] gives 12° , and Ref. [12] gives $(12 \pm 2)^\circ$, among others. Nevertheless, both smaller angles such as 5.4° [13] and much larger angles such as $(17.4 \pm 2.5)^\circ$ [14] and 40° [15] have also been reported.

Furthermore, Ref. [16] points out that the non-zero contribution of $\psi(3770)$ to the dilepton arises from two mechanisms. The first is the $S - D$ mixing induced by the tensor force, and the second originates from relativistic corrections. These two mechanisms interfere and are of the same order at v^2 . Therefore, it is generally unreasonable to consider only one mechanism while neglecting the other. Ref. [17] also indicates that the tensor force is too weak to yield a sufficiently large mixing angle, further implies that relativistic corrections must be included to explain the $S - D$ mixing of $\psi(3770)$ [4, 18]. Moreover, there is also the spin-orbit interaction in the potential, which violates total spin conservation and mixes different total spins. Since total angular momentum is conserved, this can result in, for example, $S - P$ ($P - D$) mixing, a phenomenon that has not yet been studied in detail [19].

Similar to charmonium, $S - D$ mixing must also occur in bottomonium. However, Ref. [20] points out that theoretical studies often overlook the underlying dynamic mechanisms responsible for $S - D$ mixing and artificially introduce mixing angles. This necessitates

determining mixing angles by fitting experimental data, making it difficult to study $\Upsilon(1D)$ and $\Upsilon(2D)$, for which no experimental data currently exist. Consequently, theoretical studies on their mixing are extremely limited. Therefore, it is necessary to conduct a thorough investigation into their mixings to facilitate their experimental discovery.

We note that in traditional approaches, relativistic potentials are derived by studying quark-antiquark scattering [21], where the quark spinors are expanded into non-relativistic Pauli spinors, and all quantities except the Pauli spinors are absorbed into the interaction potential, thereby obtaining a relativistic potential. In this method, the potential is relativistic, while the wave function of bound state remains non-relativistic [21]. We adopt an opposite approach: the wave function is relativistic, while the potential is non-relativistic [22, 23]. The advantage of the former is that it yields a relativistic mass spectrum, while in our approach, since we solve the instantaneous Bethe-Salpeter equation [24], both the mass spectrum and the wave function are relativistic.

The Bethe-Salpeter (BS) equation is a relativistic dynamical equation describing bound states [25]. However, similar to the Schrödinger equation, the form of the wave function is externally input. Previously, for the 1^- vector mesons, we proposed a general wave function representation in the instantaneous approximation [22, 23]. Yet this is not the only or inevitable representation. In this paper, we will present several possible relativistic wave function representations, substitute them into the BS equation for solving, and determine the optimal wave function by considering the mass spectrum and calculating annihilation decays. As an iterative integral equation, the BS equation incorporates tensor forces and relativistic corrections to infinite orders. The wave function also accounts for the mixing of different partial waves, $S - P - D$ mixing instead of only $S - D$ mixing [19].

II. INTRODUCTION OF THE SALPETER EQUATION

The BS equation is difficult to solve exactly, so we rigorously solve its instantaneous approximation, the Salpeter equation. The instantaneous approximation manifests as the interaction being independent of the time component, namely, $V(P, k, q) \sim V(\vec{k}, \vec{q}) = V(\vec{q} - \vec{k})$, where P is the total momentum of the meson, q (k) is the relative momentum between the two quarks inside the meson.

Define the positive and negative energy projection operators as $\Lambda_i^\pm(q_\perp) = \frac{1}{2\omega_i} \left[\frac{p}{M} \omega_i \pm J(i)(m_i + q_\perp) \right]$, where $J(i) = (-1)^{i+1}$, $i = 1$ for quark, and $i = 2$ for antiquark; M and m_i are the masses of meson and inside quark, respectively; $\omega_i = \sqrt{m_i^2 - q_\perp^2}$ is the energy of quark. We have defined $q_\perp \equiv q - \frac{P \cdot q}{M} P$, so $q_\perp = (0, \vec{q})$ in the center-of-mass

system of P . Applying definition, $\varphi^{\pm\pm}(q_\perp) \equiv \Lambda_1^\pm(q_\perp) \frac{\not{P}}{M} \varphi(q_\perp) \frac{\not{P}}{M} \Lambda_2^\pm(q_\perp)$, the wave function is decomposed into four terms $\varphi = \varphi^{++} + \varphi^{+-} + \varphi^{-+} + \varphi^{--}$. With these notations, the Salpeter equation is written as [24],

$$\begin{aligned} (M - \omega_1 - \omega_2) \varphi^{++}(q_\perp) &= \Lambda_1^+(q_\perp) \left[\int \frac{d\vec{k}}{(2\pi)^3} V(q_\perp - k_\perp) \varphi(k_\perp) \right] \Lambda_2^+(q_\perp), \\ (M + \omega_1 + \omega_2) \varphi^{--}(q_\perp) &= -\Lambda_1^-(q_\perp) \left[\int \frac{d\vec{k}}{(2\pi)^3} V(q_\perp - k_\perp) \varphi(k_\perp) \right] \Lambda_2^-(q_\perp), \\ \varphi^{+-}(q_\perp) &= \varphi^{-+}(q_\perp) = 0. \end{aligned} \quad (2)$$

The corresponding normalization condition is

$$\int \frac{d\vec{q}}{(2\pi)^3} \text{Tr} \left[\bar{\varphi}^{++}(q_\perp) \frac{\not{P}}{M} \varphi^{++}(q_\perp) \frac{\not{P}}{M} - \bar{\varphi}^{--}(q_\perp) \frac{\not{P}}{M} \varphi^{--}(q_\perp) \frac{\not{P}}{M} \right] = 2M, \quad (3)$$

where, $\bar{\varphi} = \gamma_0 \varphi^\dagger \gamma^0$, ‘ \dagger ’ is the Hermitian conjugate transformation.

Since the wave functions are relativistic, to avoid double counting, we must choose a non-relativistic interaction integral kernel. We adopt the modified Cornell potential [23],

$$V(\vec{q}) = -\left(\frac{\lambda}{\alpha} + V_0\right) \delta^3(\vec{q}) + \frac{\lambda}{\pi^2} \frac{1}{(\vec{q}^2 + \alpha^2)^2} - \gamma_0 \otimes \gamma^0 \frac{2}{3\pi^2} \frac{\alpha_s(\vec{q})}{(\vec{q}^2 + \alpha^2)}, \quad (4)$$

where λ is the string tension, V_0 is a free parameter, α is a small quantity to avoid infrared divergence and account for screening effects, and $\alpha_s(\vec{q}) = \frac{4\pi}{9} \frac{1}{\log(e + \vec{q}^2/\Lambda_{QCD}^2)}$ is running coupling constant, Λ_{QCD} is the QCD scale and $e = 2.7183$.

III. CHOICE OF WAVE FUNCTION REPRESENTATIONS

Similar to solving the Schrödinger equation, when solving the Salpeter equation, it is essential to first specify a concrete representation of the wave function. In quantum field theory, the general relativistic wave function of a vector meson with quantum number $J^P = 1^-$, constructed via Dirac matrices, contains 16 independent terms. However, under the instantaneous approximation, the 8 terms containing $P \cdot q \equiv P \cdot q_\perp = 0$ vanish. Consequently, the general wave function of a 1^- meson consists of 8 terms [23]:

$$\varphi_{1^-}^{\text{full}} = \epsilon \cdot q_\perp \left(f_1 + \frac{\not{P}}{M} f_2 + \frac{\not{q}_\perp}{M} f_3 + \frac{\not{P} \not{q}_\perp}{M^2} f_4 \right) + (M f_5 + \not{P} f_6) \not{\epsilon} + \left(f_7 + \frac{\not{P}}{M} f_8 \right) \not{\epsilon} \not{q}_\perp. \quad (5)$$

The radial wave functions $f_i \equiv f_i(-q_\perp^2)$ ($i = 1, 2, \dots, 8$) are functions of q_\perp^2 . By substituting the wave function Eq. (5) into the Salpeter equation for solving, we obtained numerical solutions for the mass eigenvalues and radial wave functions of various vector mesons, which were then applied to different physical processes. It was found that for S -wave-dominated

mesons such as D^* , D_s^* , J/ψ , and their radial excited states, our theoretical results align well with experimental data [22, 26–29]. However, for D -wave-dominated mesons like $\psi(3770)$, although their masses and strong decay results match experiments well [30], the annihilation results to dileptons deviates from experimental data. This indicates an unreasonable $S - D$ wave mixing in the wave function, suggesting that the expression Eq. (5) requires improvement.

In addition to parity, quarkonium also has a definite charge conjugation parity, i.e., its $J^{PC} = 1^{--}$. In Eq. (5), since the terms containing f_2 and f_7 have $C = +$, it follows that $f_2 = f_7 = 0$. We also note that the terms containing f_5 and f_6 in Eq. (5) are S -waves, the f_1 , f_2 , f_7 , and f_8 terms are P -waves, while the f_3 and f_4 terms include both S -waves and D -waves. Since $(\epsilon \cdot q_\perp) \not{q}_\perp = \frac{1}{3} q_\perp^2 \not{\epsilon} + [(\epsilon \cdot q_\perp) \not{q}_\perp - \frac{1}{3} q_\perp^2 \not{\epsilon}]$, where $\frac{1}{3} q_\perp^2 \not{\epsilon}$ is the S -wave and $(\epsilon \cdot q_\perp) \not{q}_\perp - \frac{1}{3} q_\perp^2 \not{\epsilon}$ is the D -wave [19]. So for mesons dominated by S -waves, the f_5 and f_6 terms are necessary, while for those dominated by D -waves, the f_3 and f_4 terms are required. As for a meson with $S - D$ mixing, all four terms must be included. As for the proportion of each partial wave (including P -wave) within the wave function, it is determined by the dynamic equation they satisfy, namely the Salpeter equation.

Therefore, we select the following eight choices for the relativistic wave function of the 1^{--} quarkonium,

$$\begin{aligned}
(1) \quad & \varphi_1 = \epsilon \cdot q_\perp \left(f_1 + \frac{\not{q}_\perp}{M} f_3 + \frac{\not{P} \not{q}_\perp}{M^2} f_4 \right) + (M f_5 + \not{P} f_6) \not{\epsilon} + \frac{\not{P} \not{\epsilon} \not{q}_\perp}{M} f_8, \\
(2) \quad & \varphi_2 = \epsilon \cdot q_\perp \left(f_1 + \frac{\not{q}_\perp}{M} f_3 + \frac{\not{P} \not{q}_\perp}{M^2} f_4 \right) + (M f_5 + \not{P} f_6) \not{\epsilon}, \\
(3) \quad & \varphi_3 = \epsilon \cdot q_\perp \left(\frac{\not{q}_\perp}{M} f_3 + \frac{\not{P} \not{q}_\perp}{M^2} f_4 \right) + (M f_5 + \not{P} f_6) \not{\epsilon} + \frac{\not{P} \not{\epsilon} \not{q}_\perp}{M} f_8, \\
(4) \quad & \varphi_4 = \epsilon \cdot q_\perp f_1 + (\epsilon \cdot q_\perp - \frac{1}{3} \not{\epsilon} \not{q}_\perp) \left(\frac{\not{q}_\perp}{M} f_3 + \frac{\not{P} \not{q}_\perp}{M^2} f_4 \right) + (M f_5 + \not{P} f_6) \not{\epsilon} + \frac{\not{P} \not{\epsilon} \not{q}_\perp}{M} f_8, \\
(5) \quad & \varphi_5 = \epsilon \cdot q_\perp \left(f_1 + \frac{\not{q}_\perp}{M} f_3 + \frac{\not{P} \not{q}_\perp}{M^2} f_4 \right) + \frac{\not{P} \not{\epsilon} \not{q}_\perp}{M} f_8, \\
(6) \quad & \varphi_6 = (\epsilon \cdot q_\perp - \frac{1}{3} \not{\epsilon} \not{q}_\perp) \left(\frac{\not{q}_\perp}{M} f_3 + \frac{\not{P} \not{q}_\perp}{M^2} f_4 \right) + (M f_5 + \not{P} f_6) \not{\epsilon}, \\
(7) \quad & \varphi_7 = \epsilon \cdot q_\perp f_1 + (\epsilon \cdot q_\perp - \frac{1}{3} \not{\epsilon} \not{q}_\perp) \left(\frac{\not{q}_\perp}{M} f_3 + \frac{\not{P} \not{q}_\perp}{M^2} f_4 \right) + (M f_5 + \not{P} f_6) \not{\epsilon}, \\
(8) \quad & \varphi_8 = (\epsilon \cdot q_\perp - \frac{1}{3} \not{\epsilon} \not{q}_\perp) \left(\frac{\not{q}_\perp}{M} f_3 + \frac{\not{P} \not{q}_\perp}{M^2} f_4 \right) + (M f_5 + \not{P} f_6) \not{\epsilon} + \frac{\not{P} \not{\epsilon} \not{q}_\perp}{M} f_8,
\end{aligned} \tag{6}$$

where φ_1 is the general wave function representation of the 1^{--} state, i.e., the one appears in Eq. (5). There are other possible representations for the 1^{--} wave function.

For example, $(Mf_5 + \not{P}f_6)\not{\epsilon}$ corresponds to the nonrelativistic S -wave wave function, while $(\epsilon \cdot q_\perp - \frac{1}{3}\not{\epsilon}\not{q}_\perp) \left(\frac{\not{q}_\perp}{M}f_3 + \frac{\not{P}\not{q}_\perp}{M^2}f_4 \right)$ corresponds to the nonrelativistic D -wave wave function. These choices are not relevant to our considerations and are therefore omitted.

Although the Salpeter equation places no restrictions on the representation of the wave functions, the last two sub-equations of the Eq. (2), $\varphi^{+-}(q_\perp) = \varphi^{-+}(q_\perp) = 0$, establish relations among the different radial wave functions, reducing the number of independent radial wave functions to four (two for φ_5). We choose the independent radial wave functions as f_3, f_4, f_5 , and f_6 , while the relations of the other radial wave functions to them are listed in Table I. The table also provides the corresponding normalization formulas satisfied by the radial wave functions under different choices of wave function representation.

TABLE I: Relations and normalization formulas for radial wave functions with different wave function (WF) choices.

WF	Relations	Normalization Formulas
φ_1	$f_1 = \frac{f_3 q_\perp^2 + f_5 M^2}{M m_1}, f_8 = \frac{f_6 M}{m_1}$	$\int \frac{d\vec{q}}{(2\pi)^3} \frac{4Mw_1}{3m_1} \left[3f_5 f_6 + \frac{q_\perp^2}{M^2} \left(\frac{q_\perp^2}{M^2} f_3 f_4 + f_3 f_6 + f_4 f_5 \right) \right] = 1$
φ_2	$f_1 = \frac{f_3 q_\perp^2 + f_5 M^2}{M m_1}$	$\int \frac{d\vec{q}}{(2\pi)^3} \frac{4Mw_1}{3m_1} \left[f_5 f_6 \left(3 + \frac{2q_\perp^2}{w_1^2} \right) + \frac{q_\perp^2}{M^2} \left(\frac{q_\perp^2}{M^2} f_3 f_4 + f_3 f_6 + f_4 f_5 \right) \right] = 1$
φ_3	$f_8 = \frac{f_6 M}{m_1}$	$\int \frac{d\vec{q}}{(2\pi)^3} \frac{4Mm_1}{3w_1} \left[f_5 f_6 \left(3 - \frac{2q_\perp^2}{m_1^2} \right) + \frac{q_\perp^2}{M^2} \left(\frac{q_\perp^2}{M^2} f_3 f_4 + f_3 f_6 + f_4 f_5 \right) \right] = 1$
φ_4	$f_1 = \frac{2f_3 q_\perp^2 + 3f_5 M^2}{3Mm_1}, f_8 = \frac{3f_6 M^2 - f_4 q_\perp^2}{3Mm_1}$	$\int \frac{d\vec{q}}{(2\pi)^3} \frac{4Mw_1}{m_1} \left(f_5 f_6 + \frac{2q_\perp^4}{9M^4} f_3 f_4 \right) = 1$
φ_5	$f_1 = \frac{f_3 q_\perp^2}{M m_1}, f_8 = 0$	$\int \frac{d\vec{q}}{(2\pi)^3} \frac{4q_\perp^4 w_1}{3M^3 m_1} f_3 f_4 = 1$
φ_6	—	$\int \frac{d\vec{q}}{(2\pi)^3} \frac{4Mm_1}{w_1} \left(f_5 f_6 + \frac{2q_\perp^4}{9M^4} f_3 f_4 \right) = 1$
φ_7	$f_1 = \frac{2f_3 q_\perp^2 + 3f_5 M^2}{3Mm_1}$	$\int \frac{d\vec{q}}{(2\pi)^3} \frac{4Mm_1}{3w_1} \left\{ f_5 f_6 \left(3 - \frac{q_\perp^2}{m_1^2} \right) + \frac{2q_\perp^4}{3M^4} \left[\left(1 - \frac{2q_\perp^2}{3m_1^2} \right) f_3 f_4 - \frac{M^2}{m_1^2} (f_3 f_6 + f_4 f_5) \right] \right\} = 1$
φ_8	$f_8 = \frac{3f_6 M^2 - f_4 q_\perp^2}{3Mm_1}$	$\int \frac{d\vec{q}}{(2\pi)^3} \frac{4Mm_1}{3w_1} \left\{ f_5 f_6 \left(3 - \frac{2q_\perp^2}{m_1^2} \right) + \frac{2q_\perp^4}{3M^4} \left[\left(1 - \frac{q_\perp^2}{3m_1^2} \right) f_3 f_4 + \frac{M^2}{m_1^2} (f_3 f_6 + f_4 f_5) \right] \right\} = 1$

We substitute the wave function representation containing four independent unknown radial wave functions into the first two equations of Eq. (2) for solving. Since both the equations and the wave functions contain Dirac matrices, we remove the matrices by taking the trace and find that the number of independent equations is not two on the surface but actually four. With four equations and four unknowns, the Salpeter equation can thus be solved successfully, yielding the numerical results for the radial wave functions and the mass spectrum.

The decay width of a vector quarkonium into a lepton-antilepton pair is proportional to the square of its decay constant, and the formula for calculating the decay constant F_V of a vector from its wave function is:

$$F_V M \epsilon_\mu = \sqrt{N_c} \int \frac{d^4 q}{(2\pi)^4} \text{Tr}[\chi_P(q) \gamma_\mu] = \sqrt{N_c} \int \frac{d^3 \vec{q}}{(2\pi)^3} \text{Tr}[\varphi_P(\vec{q}) \gamma_\mu], \quad (7)$$

where $N_c = 3$ is the color number. The decay constant expressions with different wave functions are presented in the last column of Table II.

IV. RESULTS AND DISCUSSION

The input parameters are fixed by fitting the mass spectra of charmonium and bottomonium with experimental data using wave function representation, φ_1 , and were not readjusted except V_0 when other wave function representations were adopted. We take $m_c = 1.60$ GeV, $m_b = 4.96$ GeV, $\alpha = 0.06$ GeV. For charmonium, $\lambda = 0.21$ GeV 2 , $\Lambda_{QCD} = 0.27$ GeV, while for bottomonium, $\lambda = 0.2$ GeV 2 , $\Lambda_{QCD} = 0.21$ GeV.

TABLE II: Charmonium mass spectrum (in unit of MeV) and decay constant formulas with different wave function (WF) choices, EX is the central value of experimental data [31].

	$M_{\psi(1S)}$	$M_{\psi(2S)}$	$M_{\psi(1D)}$	$M_{\psi(3S)}$	$M_{\psi(2D)}$	F_V
WF\EX	3096.90	3686.1	3773.7	4039	4191	
φ_1	3090.8	3683.0	3773.6	4051.4	4105.5	$4\sqrt{3} \int \frac{d\vec{q}}{(2\pi)^3} \left[f_5 - \frac{\vec{q}^2}{3M^2} f_3 \right]$
φ_2	3046.0	3667.3	3773.3	4052.2	4130.6	$4\sqrt{3} \int \frac{d\vec{q}}{(2\pi)^3} \left[f_5 - \frac{\vec{q}^2}{3M^2} f_3 \right]$
φ_3	3026.0	3633.5	3773.7	4013.0	4133.9	$4\sqrt{3} \int \frac{d\vec{q}}{(2\pi)^3} \left[f_5 - \frac{\vec{q}^2}{3M^2} f_3 \right]$
φ_4	3089.1	3681.4	3773.5	4050.0	4106.0	$4\sqrt{3} \int \frac{d\vec{q}}{(2\pi)^3} f_5$
φ_5	—	—	3773.4	—	4186.7	$-4\sqrt{3} \int \frac{d\vec{q}}{(2\pi)^3} \frac{\vec{q}^2}{3M^2} f_3$
φ_6	2978.6	3616.9	3774.0	4033.4	4138.5	$4\sqrt{3} \int \frac{d\vec{q}}{(2\pi)^3} f_5$
φ_7	3007.1	3634.6	3773.1	4043.3	4126.5	$4\sqrt{3} \int \frac{d\vec{q}}{(2\pi)^3} f_5$
φ_8	3071.4	3684.9	3773.3	4073.8	4133.4	$4\sqrt{3} \int \frac{d^3\vec{q}}{(2\pi)^3} f_5$

The calculated charmonium masses and experimental data [31] are shown in Table II. It can be seen that most of the theoretical results obtained using different wave function representations agree with the experimental data. For the Choice 5, only the mass spectrum dominated by D -wave states are obtained. This is because the input wave function φ_5 lacks a separate S -wave term, the f_3 and f_4 terms are predominantly D -wave, and the extracted S -wave is subordinate. In the other seven wave function representations, independent S -wave and D -wave terms are included, allowing the solutions to simultaneously provide solution dominated by S -wave or D -wave. It should be noted that we have only provided the wave function representations. Whether the eigenvalue is S -wave or D -wave dominant is not manually adjusted; we can only determine the nature of the state based on the wave function

solution and the mass eigenvalue.

TABLE III: Bottomonium mass spectrum (MeV) with different wave function (WF) choices, EX is the central value of experimental data [31].

	$M_{\Upsilon(1S)}$	$M_{\Upsilon(2S)}$	$M_{\Upsilon(1D)}$	$M_{\Upsilon(3S)}$	$M_{\Upsilon(2D)}$
WF\EX	9460.3	10023.26	—	10355.2	—
φ_1	9460.2	10021	10138	10362	10436
φ_2	9460.4	10031	10154	10379	10454
φ_3	9460.2	10025	10156	10370	10458
φ_4	9460.2	10021	10138	10362	10436
φ_5	—	—	10137	—	11567
φ_6	9460.1	10036	10173	10389	10477
φ_7	9460.1	10031	10164	10381	10467
φ_8	9460.9	10022	10125	10368	10429

Table III presents the corresponding mass spectrum of bottomonium. In comparison with charmonium, it can be seen that the bottomonium mass agrees perfectly with experimental data [31]. This is because bottomonium is significantly heavier, making the instantaneous approximation more suitable. It is almost impossible to determine which choice is better.

TABLE IV: The decay widths Γ (keV) of $\psi \rightarrow e^+e^-$ using wave functions (1-8).

	$\Gamma_{\psi(1S)}$	$\Gamma_{\psi(2S)}$	$\Gamma_{\psi(1D)}$	$\Gamma_{\psi(3S)}$	$\Gamma_{\psi(2D)}$
WF\EX	5.53 ± 0.10	2.33 ± 0.04	0.262 ± 0.018	0.86 ± 0.07	0.48 ± 0.22
φ_1	$8.49^{+0.72}_{-0.68}$	$3.94^{+0.27}_{-0.24}$	$0.054^{+0.015}_{-0.011}$	$2.57^{+0.14}_{-0.13}$	$0.088^{+0.028}_{-0.020}$
φ_2	$8.91^{+0.74}_{-0.70}$	$3.38^{+0.10}_{-0.10}$	$0.231^{+0.091}_{-0.067}$	$1.22^{+0.18}_{-0.16}$	$0.986^{+0.240}_{-0.221}$
φ_3	$12.8^{+1.5}_{-1.3}$	$6.51^{+0.55}_{-0.53}$	$0.378^{+0.151}_{-0.110}$	$3.69^{+0.13}_{-0.16}$	$1.31^{+0.42}_{-0.32}$
φ_4	$8.46^{+0.74}_{-0.66}$	$3.94^{+0.23}_{-0.25}$	$0.144^{+0.041}_{-0.031}$	$2.57^{+0.13}_{-0.14}$	$0.210^{+0.066}_{-0.049}$
φ_5	—	—	$1.54^{+0.07}_{-0.08}$	—	$0.400^{+0.000}_{-0.003}$
φ_6	$14.5^{+1.7}_{-1.6}$	$6.96^{+0.73}_{-0.65}$	$0.087^{+0.024}_{-0.019}$	$4.68^{+0.45}_{-0.41}$	$0.126^{+0.033}_{-0.026}$
φ_7	$8.73^{+0.71}_{-0.67}$	$3.71^{+0.20}_{-0.21}$	$0.0019^{+0.0005}_{-0.0006}$	$2.30^{+0.08}_{-0.09}$	$0.0019^{+0.0026}_{-0.0013}$
φ_8	$7.46^{+0.58}_{-0.55}$	$3.39^{+0.20}_{-0.19}$	$0.058^{+0.015}_{-0.012}$	$2.34^{+0.16}_{-0.14}$	$0.074^{+0.020}_{-0.016}$

Using the decay constant formulas given in Table II, we calculate the annihilation of quarkonia into dileptons, with the results listed in Tables IV and V. As shown in Table IV,

although it is difficult to determine the best wave function representation solely by the mass spectrum, the partial widths to dileptons provide a clear answer. If only considering states dominated by S -waves, selecting wave functions φ_1 , φ_2 , φ_4 , φ_7 , and φ_8 can all yield results that consistent with experiments. However, when also comprehensively considering states dominated by D -waves, only the φ_2 produces the results, $\Gamma(\psi(3770) \rightarrow e^+e^-) = 0.231^{+0.091}_{-0.067}$ keV and $\Gamma(\psi(4160) \rightarrow e^+e^-) = 0.986^{+0.240}_{-0.221}$ keV, that match the PDG data $\Gamma_{\psi(3770)}^{\text{EX}} = 0.262 \pm 0.018$ keV and $\Gamma_{\psi(4160)}^{\text{EX}} = 0.48 \pm 0.22$ keV [31]. Our result of $\psi(4160)$ is in good agreement with the experimental value of 0.83 ± 0.07 keV in Ref. [32]. We note that the center value of $\Gamma_{\psi(4160) \rightarrow \mu^+\mu^-}^{\text{EX}} = 2.45 \pm 1.24 \pm 0.94$ keV in recent experiment is quite large [31], indicating the dilepton process of $\psi(4160)$ still requires more precise experimental investigation. Our theoretical error is obtained by varying all parameters by $\pm 5\%$ arbitrarily.

TABLE V: The decay widths Γ (keV) of $\Upsilon \rightarrow e^+e^-$ using wave functions (1-8).

	$\Gamma_{\Upsilon(1S)}$	$\Gamma_{\Upsilon(2S)}$	$\Gamma_{\Upsilon(1D)} \times 10^{-3}$	$\Gamma_{\Upsilon(3S)}$	$\Gamma_{\Upsilon(2D)} \times 10^{-3}$
WF \ EX	1.340 ± 0.018	0.612 ± 0.011	-	0.443 ± 0.008	-
φ_1	$1.29^{+0.09}_{-0.08}$	$0.630^{+0.048}_{-0.046}$	$0.748^{+0.232}_{-0.150}$	$0.447^{+0.034}_{-0.032}$	$1.18^{+0.36}_{-0.24}$
φ_2	$1.32^{+0.10}_{-0.06}$	$0.610^{+0.043}_{-0.042}$	$2.29^{+0.86}_{-0.69}$	$0.412^{+0.028}_{-0.027}$	$10.5^{+4.2}_{-3.1}$
φ_3	$1.56^{+0.11}_{-0.14}$	$0.788^{+0.074}_{-0.068}$	$2.98^{+1.24}_{-0.86}$	$0.564^{+0.051}_{-0.047}$	$12.5^{+4.9}_{-3.5}$
φ_4	$1.29^{+0.09}_{-0.09}$	$0.628^{+0.049}_{-0.046}$	$2.55^{+0.66}_{-0.52}$	$0.446^{+0.034}_{-0.032}$	$3.15^{+0.91}_{-0.65}$
φ_5	—	—	2330^{+80}_{-80}	—	195^{+7}_{-8}
φ_6	$1.61^{+0.08}_{-0.12}$	$0.778^{+0.054}_{-0.067}$	$0.876^{+0.204}_{-0.202}$	$0.556^{+0.042}_{-0.048}$	$1.44^{+0.36}_{-0.32}$
φ_7	$1.27^{+0.05}_{-0.05}$	$0.590^{+0.033}_{-0.029}$	$0.297^{+0.002}_{-0.005}$	$0.412^{+0.022}_{-0.023}$	$0.262^{+0.050}_{-0.059}$
φ_8	$0.803^{+0.063}_{-0.061}$	$0.362^{+0.032}_{-0.032}$	$0.451^{+0.247}_{-0.006}$	$0.238^{+0.024}_{-0.031}$	$0.926^{+0.136}_{-0.490}$

As shown in Table V for the annihilation decay results of bottomonium, if only the S -wave dominated states are considered, wave functions φ_1 , φ_2 , φ_4 , and φ_7 can all yield results consistent well with experimental data [31]. However, we believe that the same wave function representation should be adopted for both charmonium and bottomonium. Therefore, we propose selecting wave function φ_2 , for the D -wave dominated states, we obtain $\Gamma(\Upsilon(1D) \rightarrow e^+e^-) = 2.29^{+0.86}_{-0.69}$ eV and $\Gamma(\Upsilon(2D) \rightarrow e^+e^-) = 10.5^{+4.2}_{-3.1}$ eV.

For comparison, we present in Table VI the results calculated using wave function φ_2 as well as results from other theories. As can be seen, we have provided the largest decay width, especially the $2D$ result, which is several times larger than other theoretical results. Apart from Refs. [33] and [20], which account for $S - D$ mixing by incorporating tensor force and coupled-channel effects respectively, other theoretical calculations have neglected the

mixing effect. From the results, even when mixing effects are considered, the predictions in Refs. [33] and [20] remain very close to other theoretical values, indicating that the mixing effect in these two papers is minimal. This observation is inconsistent with our findings, particularly regarding the $2D$ results.

TABLE VI: Dilepton decay widths (eV), ours are obtained using the wave function φ_2

	ours	[33]	[34]	[35]	[36]	[37]	[38]	[39]	[20]
$\Gamma(\Upsilon(1D) \rightarrow e^+ e^-)$	$2.29^{+0.86}_{-0.69}$	1.5	0.37	0.62	1.38	1.4	1.88	1.65	1.08
$\Gamma(\Upsilon(2D) \rightarrow e^+ e^-)$	$10.5^{+4.2}_{-3.1}$	2.7	0.58	1.08	1.99	2.5	2.81	2.42	2.13

Next, we discuss the mixing problem. Unlike the commonly adopted approach, we do not separately solve for the S -wave and D -wave wave functions and artificially mix them using Eq. (1), with the undetermined mixing angle fitted to experimental values. Instead, we present a wave function representation for the 1^{--} state that simultaneously contains S -wave, P -wave, and D -wave components, where the relative proportions of different waves are determined by the dynamical Sapeter equation satisfied by the wave function.

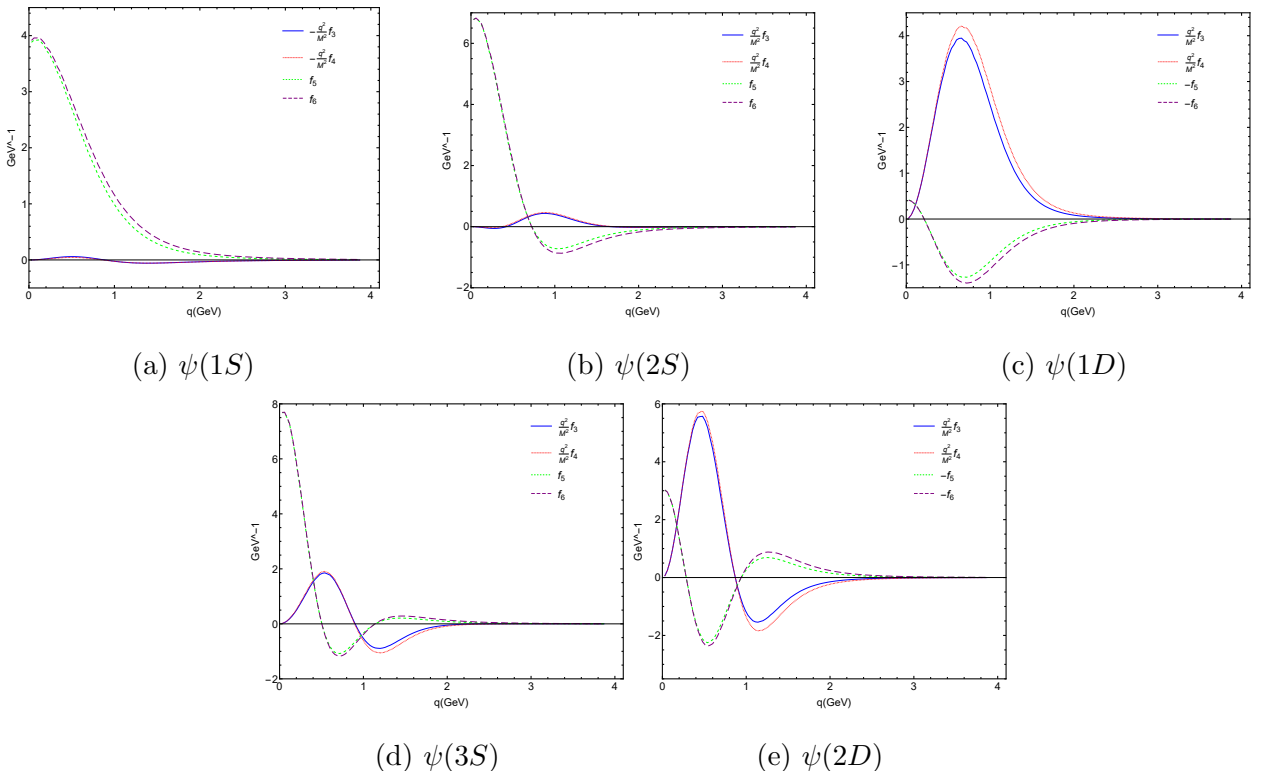


FIG. 1: Radial wave functions of the wave function φ_2 for charmonium, where $q \equiv |\vec{q}|$.

We illustrate this using only charmonium wave function φ_2 as an example. The independent radial wave functions corresponding to the first five eigen states are plotted in Fig.

1. In Fig. 1(a), the S -wave radial wave functions f_5 and f_6 dominate and have no nodes, indicating that this state is the $1S$ state $\psi(1S)$. Its wave function contains a very small admixture of D -wave from f_3 and f_4 , which manifests as a $2D$ -wave. In Fig. 1(b), the dominant S -wave has one node, identifying it as the $2S$ state $\psi(2S)$, while the mixed D -wave component overall exhibits the behavior of a $1D$ -wave. In Fig. 1(c), f_3 and f_4 dominate and show no nodes, thus corresponding to the $1D$ state $\psi(1D)$ mixed with a $2S$ -wave. In Fig. 1(d), the $3S$ -wave is dominant and mixed with a $2D$ -wave, so it is the $\psi(3S)$; whereas the fifth state in Fig. 1(e) is predominantly a $2D$ -wave mixed with a $3S$ -wave, corresponding to $\psi(2D)$ state.

In addition to the S -wave and D -wave, the 1^{--} wave function in our method also contains a P -wave component. Rather than plotting its radial wave function, we instead present the proportions of the S -, P -, and D -wave components in each state based on the normalized wave function formula. For wave function φ_2 , the results are listed in Table VII. We conclude that in the $1S$, $2S$, and $3S$ states, the S -wave dominates and provides the non-relativistic contribution, the P -wave and D -wave supply the relativistic correction. In the $1D$ and $2D$ states, the D -wave is dominant and provides the non-relativistic contribution, the S -wave and P -wave contribute the relativistic corrections. Comparing the ratios of $S : P : D$ reveals that the relativistic corrections in bottomonium are much smaller than those in charmonium. Furthermore, it can also be seen from the $S : D$ ratios that the mixing angles in bottomonium are significantly smaller than those in charmonium.

TABLE VII: Partial wave ratios $S : P : D$ in the wave function φ_2 for heavy quarkonium

	$1S$	$2S$	$1D$	$3S$	$2D$
ψ	$1 : 0.0639 : 0.0281$	$1 : 0.180 : 0.117$	$0.139 : 0.221 : 1$	$1 : 0.252 : 0.483$	$0.495 : 0.339 : 1$
Υ	$1 : 0.0257 : 0.0137$	$1 : 0.0339 : 0.0208$	$0.0310 : 0.0499 : 1$	$1 : 0.0617 : 0.0816$	$0.0953 : 0.0726 : 1$

If we ignore the contribution of the P -wave and follow the relation given in the first formula in Eq.(1) to calculate the $S - D$ mixing angle for $2S$ and $3S$ states, and the second formula to calculate the mixing angle for $1D$ and $2D$ states under different wave function choices. The results are presented in Table VIII. As can be seen, the mixing angles we obtained for $2S$ and $1D$ states, as well as for $3S$ and $2D$ states, are generally different. For example, adopting φ_2 , $\theta_{2S} = (6.67^{+1.71}_{-1.50})^\circ$ is obtained for $\psi(2S)$, while for $\psi(1D)$ it is $\theta_{1D} = (7.92^{+1.70}_{-1.43})^\circ$. The latter is quite close to the ones from the simple $2S - 1D$ mixing scheme: 10° [10], 12° [11], and $(12 \pm 2)^\circ$ [12]. For the $2D$ state $\psi(4160)$, as a $3S - 2D$ mixing state, $\theta_{2D} = (26.3^{+3.3}_{-3.4})^\circ$ is obtained, which confirms the large mixing angle of 35° in Ref.

[40], 34.8° in Ref. [41], and 21.2° in Ref. [42].

TABLE VIII: The $S - D$ mixing angle θ ($^\circ$) of charmonium and bottomonium with neglected the P -wave using wave functions (1-8).

WF	$\theta_{\psi(2S)}$	$\theta_{\psi(1D)}$	$\theta_{\psi(3S)}$	$\theta_{\psi(2D)}$	$\theta_{\Upsilon(2S)}$	$\theta_{\Upsilon(1D)}$	$\theta_{\Upsilon(3S)}$	$\theta_{\Upsilon(2D)}$
φ_1	$3.66^{+0.06}_{-0.15}$	$3.65^{+0.27}_{-0.25}$	$4.02^{+0.23}_{-0.22}$	$4.01^{+0.16}_{-0.21}$	$1.44^{+0.11}_{-0.10}$	$1.16^{+0.10}_{-0.10}$	$1.56^{+0.12}_{-0.12}$	$1.41^{+0.12}_{-0.12}$
φ_2	$6.67^{+1.71}_{-1.50}$	$7.92^{+1.70}_{-1.43}$	$25.8^{+3.0}_{-3.7}$	$26.3^{+3.3}_{-3.4}$	$1.19^{+0.22}_{-0.04}$	$1.78^{+0.32}_{-0.25}$	$4.67^{+0.85}_{-0.65}$	$5.44^{+1.10}_{-0.76}$
φ_3	$4.45^{+0.77}_{-0.80}$	$5.97^{+0.73}_{-0.69}$	$13.7^{+1.3}_{-1.2}$	$14.6^{+1.0}_{-1.2}$	$1.12^{+0.19}_{-0.18}$	$1.68^{+0.26}_{-0.20}$	$3.97^{+0.59}_{-0.58}$	$4.61^{+0.62}_{-0.54}$
φ_4	$4.53^{+0.32}_{-0.20}$	$3.66^{+0.18}_{-0.22}$	$5.01^{+0.37}_{-0.32}$	$6.23^{+1.60}_{-1.32}$	$1.58^{+0.13}_{-0.12}$	$0.857^{+0.266}_{-0.453}$	$1.72^{+0.14}_{-0.14}$	$1.40^{+0.11}_{-0.11}$
φ_5	—	35.3 ± 0	—	35.3 ± 0	—	35.3 ± 0	—	35.3 ± 0
φ_6	$4.42^{+0.33}_{-0.31}$	$4.33^{+0.41}_{-0.37}$	$4.96^{+0.37}_{-0.33}$	$5.06^{+0.43}_{-0.40}$	$1.52^{+0.11}_{-0.11}$	$1.20^{+0.10}_{-0.10}$	$1.67^{+0.12}_{-0.13}$	$1.49^{+0.12}_{-0.13}$
φ_7	$7.30^{+0.01}_{-0.08}$	$7.51^{+0.30}_{-0.28}$	$7.55^{+0.17}_{-0.29}$	$8.46^{+0.10}_{-0.10}$	$3.81^{+0.21}_{-0.12}$	$3.27^{+0.18}_{-0.12}$	$4.99^{+0.21}_{-0.08}$	$4.56^{+0.23}_{-0.07}$
φ_8	$11.9^{+0.38}_{-0.20}$	$3.49^{+0.25}_{-0.24}$	$10.6^{+0.4}_{-0.7}$	$3.36^{+0.26}_{-0.24}$	$4.56^{+0.54}_{-1.50}$	$1.13^{+0.13}_{-0.11}$	$4.62^{+2.30}_{-0.93}$	$1.35^{+0.11}_{-0.81}$

For bottomonium, the mixing angles we obtained using φ_2 are ($\theta_{\Upsilon(1D)}$) = ($1.78^{+0.32}_{-0.25}$), ($\theta_{\Upsilon(2D)}$) = ($5.44^{+1.10}_{-0.76}$), which are significantly larger than the results from Ref. [43] using the coupled-channel approach, (0.02° , 0.27°). Ref. [17] also chose the coupled-channel method, if we apply their data and only account for $2S - 1D$ and $3S - 2D$ mixings while ignoring other mixings, their mixing angles are (2.63° , 5.60°), which align well with ours. In addition to small mixing angles, Ref. [42] reports large mixing angles, (9° , 12.5°). Due to the absence of experimental data for the $1D$ and $2D$ states, they determined the mixing angles by fitting only the dilepton decays of the $2S$ and $3S$ states. However, as known that the S -wave component in the $1D$ state contributes the majority of the dilepton partial width, while the D -wave component has only a minor effect on the partial width of the $2S$ state. Considering other influences such as relativistic and QCD corrections, extracting mixing angles solely by fitting the $2S$ and $3S$ states makes it difficult to control the errors.

V. CONCLUSION

This paper systematically investigates eight different relativistic wave function representations by solving the instantaneous BS equation, with a focus on exploring the $S - D$ mixing in vector charmonium and bottomonium states.

We find that the choice of wave function representation is crucial. Among the eight candidate wave functions, the φ_2 representation provides the most consistent description of the experimentally observed mass spectra and dileptonic decay widths. This representation

not only accurately reproduces the properties of S -wave dominant states (such as $\psi(1S - 3S)$, $\Upsilon(1S - 3S)$), but also successfully predicts the decay behaviors of D -wave dominant states (such as $\psi(3770)$ and $\psi(4160)$), with theoretical calculations in good agreement with experimental data. Based on this, we predict the decay widths of the yet-unobserved $\Upsilon(1D)$ and $\Upsilon(2D)$ states.

$S - P - D$ mixing is a universal phenomenon: Our analysis shows that the wave functions of vector mesons are not simple $S - D$ mixtures but contain significant P -wave components, forming $S - P - D$ mixing. For example, in the $\psi(2S)$ state, the proportions of S , P , and D waves are approximately $1 : 0.18 : 0.12$; in the $\psi(3770)$, the ratio is about $0.14 : 0.22 : 1$. Such mixing is naturally determined by the dynamics of the Salpeter equation, reflecting the inherent requirements of relativistic effects.

Based on calculations using the wave function φ_2 , we obtain more reasonable mixing angles. For charmonium, the mixing angle of $\psi(3770)$ is $(7.92^{+1.70}_{-1.43})^\circ$, and that of $\psi(4160)$ is $(26.3^{+3.3}_{-3.4})^\circ$. The mixing angles in bottomonium are much smaller than those in charmonium, such as $(1.78^{+0.32}_{-0.25})^\circ$ for $\Upsilon(1D)$ and $(5.44^{+1.10}_{-0.76})^\circ$ for $\Upsilon(2D)$, owing to the heavier mass of the bottom quark, which reduces relativistic effects.

This paper predicts the dileptonic decay widths of the bottomonium states $\Upsilon(1D)$ and $\Upsilon(2D)$ to be $(2.29^{+0.86}_{-0.69})$ eV and $(10.5^{+4.2}_{-3.1})$ eV, respectively. These values are larger than existing theoretical results, and future experimental measurements will help verify the reliability of this model.

In summary, by optimizing the wave function representation, this study achieves an accurate description of $S - P - D$ mixing in vector quarkonia within the Salpeter equation framework, emphasizing the importance of relativistic corrections and multi-wave mixing. The results provide valuable theoretical references for future experimental studies of related particles.

Acknowledgments This work was supported by the National Natural Science Foundation of China (NSFC) under the Grants No. 12575097, No. 12075073, and No. 12375085. Q. Li was supported by the National Key R&D Program of China (2022YFA1604803) and the Natural Science Basic Research Program of Shaanxi (No. 2025JC-YBMS-020). T. Wang was supported by the Fundamental Research Funds for the Central Universities (2023FRFK06009).

[1] P. A. Rapidis, et al., Phys. Rev. Lett. **39**, 526 (1977), Phys. Rev. Lett. **39**, 974 (1977) (erratum).

[2] E. Eichten, K. Gottfried, T. Kinoshita, J. Kogut, K. D. Lane, and T.-M. Yan, Phys. Rev. Lett. **34**, 369 (1975), Phys. Rev. Lett. **36**, 1276 (1976) (erratum).

[3] E. Eichten, K. Gottfried, T. Kinoshita, K. D. Lane, and T.-M. Yan, Phys. Rev. D **17**, 3090 (1978).

[4] E. Eichten, K. Gottfried, T. Kinoshita, K. D. Lane, and T. M. Yan, Phys. Rev. D **21**, 203 (1980).

[5] E. Eichten, K. Lane, and C. Quigg, Phys. Rev. D **69**, 094019 (2004).

[6] E. Eichten, K. Lane, and C. Quigg, Phys. Rev. D **73**, 014014 (2006).

[7] J.-B. Liu, and M.-Z. Yang, JHEP **07**, 106 (2014).

[8] H. Yamamoto, A. Nishimura, and Y. Yamaguchi, Prog. Theor. phys. **54**, 374 (1977).

[9] E. Eichten, S. Godfrey, H. Mahlke and J. L. Rosner, Rev. Mod. Phys. **80**, 1161 (2008).

[10] Y.-B. Ding, D.-H. Qin and K.-T. Chao, Phys. Rev. D **44**, 3562 (1991).

[11] Y.-P. Kuang, Phys. Rev. D **65**, 094024 (2002).

[12] J. L. Rosner, Annals Phys. **319**, 1 (2005).

[13] Y.-J. Zhang, and Q. Zhao, Phys. Rev. D **81**, 034011 (2010).

[14] T. Barnes, S. Godfrey and E. S. Swanson, Phys. Rev. D **72**, 054026 (2005).

[15] K. Y. Liu and K. T. Chao, Phys. Rev. D **70**, 094001 (2004).

[16] M. B. Voloshin, Prog. Part. Nucl. Phys. **61**, 455 (2008).

[17] K. Heikkilä, N. A. Törnqvist, and S. Ono, Phys. Rev. D **29**, 110 (1984), Phys. Rev. D **29**, 2136 (1984) (erratum).

[18] V. A. Novikov, L. B. Okun, M. A. Shifman, A. I. Vainshtein, M. B. Voloshin, and V. I. Zakharov, Phys. Rep. **41**, 1 (1978).

[19] S.-Y. Pei, W. Li, T.-T. Liu, M. Han, G.-L. Wang, and T. Wang, Phys. Rev. D **108**, 033003 (2023).

[20] R.-H. Ni, Q. Deng, J.-J. Wu, and X.-H. Zhong, Phys. Rev. D **111**, 114027 (2025).

[21] S. N. Gupta, and S. F. Radford, Phys. Rev. D **24**, 2309 (1981).

[22] G.-L. Wang, and X.-G. Wu, Chin. Phys. C **44**, 063104 (2020).

[23] G.-L. Wang, Phys. Lett. B **633**, 492 (2006).

[24] E. E. Salpeter, Phys. Rev. **87**, 328 (1952).

[25] E. E. Salpeter and H. A. Bethe, Phys. Rev. **84**, 1232 (1951).

[26] H.-F. Fu, G.-L. Wang, Z.-H. Wang, and X.-J. Chen, Chin. Phys. Lett. **28**, 121301 (2011).

[27] X.-J. Chen, H.-F. Fu, C. S. Kim, and G.-L. Wang, J. Phys. G **39**, 045002 (2012).

[28] S.-Y. Pei, W. Li, T. Wang, and G.-L. Wang, JHEP **08**, 191 (2024).

[29] M. Jia, W. Li, S.-Y. Pei, X.-Y. Du, G.-Z. Ning, and G.-L. Wang, Eur. Phys. J. C **85**, 282

(2025).

- [30] C.-H. Chang, and G.-L. Wang, *Sci. China Phys. Mech. Astron.* **53**, 2005 (2010).
- [31] S. Navas *et al.* (Particle Data Group), *Phys. Rev. D* **110**, 030001 (2024).
- [32] K. K. Seth, *Phys. Rev. D* **72**, 017501 (2005).
- [33] P. Moxhay, and J. L. Rosner, *Phys. Rev. D* **28**, 1132 (1983).
- [34] P. Gonzalez, A. Valcarce, H. Garcilazo, and J. Vijande, *Phys. Rev. D* **68**, 034007 (2003).
- [35] A. M. Badalian, B. L. G. Bakker, and I. V. Danilkin, *Phys. Rev. D* **79**, 037505 (2009).
- [36] S. Godfrey, and K. Moats, *Phys. Rev. D* **92**, 054034 (2015).
- [37] J. Segovia, P. G. Ortega, D. R. Entem, and F. Fernandez, *Phys. Rev. D* **93**, 074027 (2016).
- [38] J.-Z. Wang, Z.-F. Sun, X. Liu, and T. Matsuki, *Eur. Phys. J. C* **78**, 915 (2018).
- [39] V. Kher, R. Chaturvedi, N. Devlani, and A. K. Rai, *Eur. Phys. J. Plus* **137**, 357 (2022).
- [40] K.-T. Chao, *Phys. Lett. B* **661**, 348 (2008).
- [41] A. M. Badalian, B. L. G. Bakker, and I. V. Danilkin, *Phys. Atom. Nucl.* **72**, 638 (2009).
- [42] Z. Zhao, K. Xu, A. Limphirat, W. Sreethawong, N. Tagsinsit, A. Kaewsnod, X. Liu, K. Khosonthongkee, S. Cheedket, and Y. Yan, *Phys. Rev. D* **109**, 016012 (2024).
- [43] Y. Lu, M. N. Anwar, and B.-S. Zou, *Phys. Rev. D* **94**, 034021 (2016).